DOI: 10.1002/ejoc.200500626

A Novel Bis(zinc–porphyrin)–Oxoporphyrinogen Donor–Acceptor Triad: Synthesis, Electrochemical, Computational and Photochemical Studies

Jonathan P. Hill,*[a] Atula S. D. Sandanayaka,[b] Amy L. McCarty,[c] Paul A. Karr,[c] Melvin E. Zandler,[c] Richard Charvet,[a] Katsuhiko Ariga,[d] Yasuyuki Araki,[b] Osamu Ito,*[b] and Francis D'Souza*[c]

Keywords: Porphyrin / Oxoporphyrinogen / Photochemistry / Electrochemistry

The first example of a porphyrin-quinonoid donor–acceptor triad featuring (tetraphenylporphinato)zinc(II) moieties covalently attached to an oxoporphyrinogen through its macrocyclic nitrogen atoms is reported. This arrangement of chromophores results in an interesting interplay between the electron-donating zinc–porphyrin(s) and the electron/energy accepting oxoporphyrinogen. The optical absorption of the triad reveals features corresponding to both the donor and acceptor entities. The geometry and electronic structure of the triad deduced from B3LYP/3-21G(*) calculations reveal an absence of inter-chromophoric interactions and localization of the HOMO on one zinc–porphyrin group and the LUMO on the oxoporphyrinogen scaffold. The electrochemical redox states of the triad were established from a comparative electrochemistry of the triad and the reference compounds. Both steady-state and time-resolved emission studies revealed quenching of the singlet excited state of zinc–porphyrin in the triad, and the free-energy calculations performed using Weller's approach indicate the possibility of electron transfer from the singlet excited zinc–porphyrin group to the oxoporphyrinogen in polar solvents. Time-resolved fluorescence studies reveal excited state energy transfer from zinc–porphyrin to oxoporphyrinogen in nonpolar solvents, while nanosecond transient absorption studies combined with time-resolved fluorescence studies in polar solvents are indicative of the occurrence of photoinduced charge separation from the singlet excited zinc–porphyrin to the oxoporphyrinogen.

Introduction

The concept of a quinone-linked porphyrin was originally introduced to model the photochemical processes occurring in photosynthetic systems.[1] This concept has since been adopted in work involving a wider variety of molecular components.[2] The archetypal molecule consists of a zinc–porphyrin covalently linked to a quinone moiety, and this has appeared frequently in a variety of guises, even containing multiple porphyrin or quinone groups.[3] Apart from the mere presence of these electron donating and electron accepting components, it was recognized that the inter-component distance and orientation has a crucial effect on the photophysical properties of these systems, just as it is in natural photosynthetic systems, so that often intricate syntheses have been performed to obtain molecules where the tetrapyrrole and quinone are in the required configuration.[4] One notable extension to the family of donor–acceptor molecules has been in the replacement of the quinone group with a fullerene acceptor[5] because of an ostensible improvement in electron-accepting properties and the stability of its reduced species.[6] Further to their importance and relevance as photosynthetic model compounds, such molecules are implicated as potential device components in molecular electronics and photovoltaics.[7] This is related to the fact that the σ-bonded arrangement of electron donor and electron acceptor permits these compounds to exist in a variety of stable oxidation states and as charge-separated species on ultrafast time scales.

Porphyrinogen species containing macrocyclic conjugation pathways have been observed previously in the structures of *meso*-tetramethylene-porphyrinogen (**1**)[8] and *meso*-tetraoxo-octaethylporphyrin (**2**)[9] (which is known trivially as xanthoporphyrinogen) (Scheme 1). Thus, oxoporphyrinogen **3** (OxP) can be considered as the cyclohexadienylidene analogue of **2**.[10] Having shown that the oxoporphyrinogen, **3** and its *N*-alkylated derivatives (such as **4**) are electron deficient and can exist in a variety of redox states,[11,12] we were interested in building higher function into derivatives of **3** by incorporating appropriate

[a] International Center for Young Scientists, National Institute for Materials Science,
Namiki 1-1, Tsukuba 305-0044, Ibaraki, Japan
[b] Institute of Multidisciplinary Research for Advanced Materials, Tohoku University,
CREST (JST), Katahira, Aoba-ku, Sendai, 980-8577 Japan
[c] Department of Chemistry, Wichita State University,
1845 Fairmount, Wichita, Kansas 67260-0051, USA
[d] Supermolecules Group, Advanced Materials Laboratory, National Institute for Materials Research,
Namiki 1-1, Tsukuba, Ibaraki 305-0044, Japan
Supporting information for this article is available on the WWW under http://www.eurjoc.org or from the author.

modular species, especially those related to light energy harvesting applications. Thus, the bis(zinc–porphyrin)–oxoporphyrinogen [$(ZnTPP)_2$-OxP] (**5**), was prepared as an example of a donor–acceptor type triad. We demonstrate here that, upon excitation of the zinc–porphyrin(s), an efficient energy or electron transfer occurs in this novel triad, and that this depends on the polarity of the solvent used in the studies.

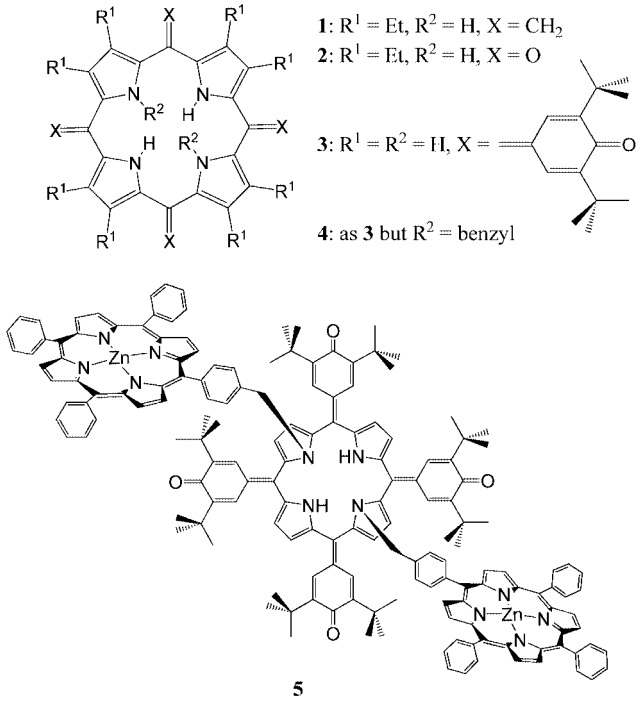

Scheme 1. Structure of the porphyrinogens, **1**–**4** and the bis(zinc–porphyrin)–oxoporphyrinogen triad **5**.

Results and Discussion

The methodology adopted for the synthesis of triad **5** is an extension of the previous work on **3**[11–13] and required the initial synthesis of a bromomethyl-substituted tetraphenylporphyrin and its subsequent use in *N*-alkylation of **3** yielding the required triad **5**. For **5**, *N*-alkylation of the porphyrinogen **3** consistently occurs in a stepwise manner and without altering the conformation of the macrocycle. Figure 1 shows the X-ray structure of the N^{21},N^{23}-benzylated oxoporphyrinogen **4** as an example.[11] All known di-*N*-substituted derivatives of **3** exist in this configuration because of the apparent direction of the subsequent *N*-alkylating group to N^{23} in the mono-*N*-substituted derivative. Thus, a structure analogous with that of **4** is assigned to compound **5**, and was confirmed by NMR and computational studies. Notably, the presence of only two *tert*-butyl proton resonances in the NMR spectrum of **5** excludes the possibility of less symmetrical isomers of the triad (see Exp. Sect. for NMR spectroscopic data).

The electronic spectra of ZnTPP, **3** and **5** are shown in Figure 2. Compound **3** exhibits a broad absorption maximum at 518 nm, occupying most of the UV and visible region of the spectrum and this broad, red-shifted spectrum for oxoporphyrinogen (relative to porphyrin) has been attributed to the extended conjugation of the macrocycle to include its *meso*-substituents.[11] As a consequence of *N*-substitution at N^{21} and N^{23} in **5**, there is a nearly 10 nm blue shift of the oxoporphyrinogen absorption maximum with the loss of a tail in the longer wavelength than 650 nm. This is due to the increasing steric bulk at the oxoporphyrinogen core and the consequent slight reduction in overlap between unsaturated groups. There is no appreciable shift in the Soret band position of the ZnTPP entity of **5**, when compared to pristine ZnTPP, indicating that there is little or no electronic interchromophore interaction between identical or non-identical moieties within **5**. Intensity of the 420 nm band of **5** is less than that of ZnTPP, which is only a sign of the weak interaction between the ZnTPP units and the **3** unit in **5**. Thus, the electronic absorption spectrum is essentially the superimposition of the spectra due to ZnTPP and an N^{21},N^{23}-dibenzyloxoporphyrinogen such as **4**. This lack of intramolecular interaction between N-substituents is expected because of the restricted rotation at the methyl-

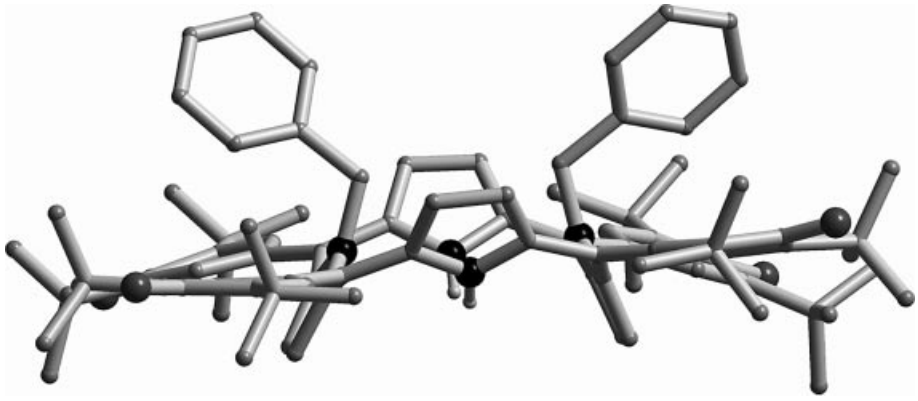

Figure 1. X-ray structure of N^{21},N^{23}-dibenzyl-5,10,15,20-(3,5-di-*tert*-butyl-4-oxocyclohexa-2,5-dienylidene)porphyrinogen (**4**) (from ref.[11]). (key: C, small, light grey sphere; N, black; O, dark grey).

ene group adjoining the two different components of **5**. This has been noted in the *N*-naphth-2-ylmethyl derivatives where intermolecular interactions are preferred.[12]

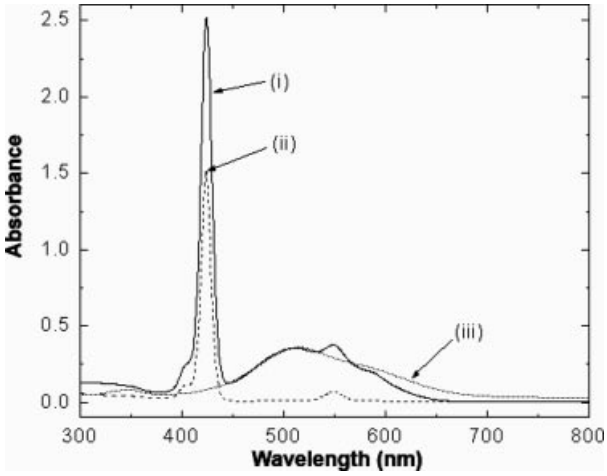

Figure 2. Absorption spectrum of (i) **5** (solid line), (ii) ZnTPP (dashed line), and (iii) **3** (dotted line) in *o*-dichlorobenzene.

Electrochemical studies were performed to evaluate the redox potentials and energetics of different photochemical processes. Figure 3 shows the cyclic voltammograms of **3** and **5** in *o*-dichlorobenzene containing 0.1 M $(n\text{Bu})_4\text{NClO}_4$. The reference compound ZnTPP undergoes two one-electron oxidations located at 0.28 and 0.62 V vs. Fc/Fc^+ corresponding to the formation of a zinc–porphyrin cation radical and a dication species, respectively, and two one-electron reductions located at –1.92 and –2.23 V vs. Fc/Fc^+ corresponding to the formation of a zinc–porphyrin anion radical and a dianion species, respectively.[5c] The cyclic voltammogram of the oxoporphyrinogen **3** exhibits two reversible oxidations located at $E_{1/2}$ = 0.27 and 0.48 V vs. Fc/Fc^+ corresponding to the formation of cation radical and dication species, respectively, and an irreversible reduction at E_{pc} = –1.33 V vs. Fc/Fc^+. The current for the reduction process is twice that for the individual oxidation processes, suggesting the occurrence of a two-electron reduction process. This two-electron reduction is conceivable since the conversion of the oxoporphyrinogen to its parent (4-hydroxyphenyl)-porphyrin (or vice versa) involves a two-electron, two-proton process.[12]

Introduction of *N*-alkyl substituents at the oxoporphyrinogen macrocycle results in anodic shifts of the oxidation potentials without significant alteration of its reduction potentials.[11,12] However, the same substitution causes the two-electron irreversible reduction process to become two one-electron reversible processes. Generally, for each added *N*-alkyl substituent (alkyl = benzyl or naphth-2-ylmethyl) an anodic shift of nearly 100 mV is observed.[11,12] This is also the case for the triad **5** substituted at N^{21} and N^{23} with zinc–porphyrins. As shown in Figure 3, the first oxidation of the oxoporphyrinogen coincides with the second oxidation of the zinc–porphyrin and appears at around 0.50 V vs. Fc/Fc^+. The oxidation potentials corresponding to the zinc–porphyrin (each is an overlapping two one-electron process because of the presence of two zinc–porphyrins) are located at 0.28 and 0.64 V vs. Fc/Fc^+ and do not vary from pristine ZnTPP. The reductions corresponding to the oxoporphyrinogen of **5** are located at –1.33 and –1.48 V vs. Fc/Fc^+. The first and second reductions of the zinc–porphyrins are located at –1.94 and –2.29 V vs. Fc/Fc^+, respectively. The HOMO–LUMO gap, measured as the potential difference between the first oxidation of the donor, zinc–porphyrin entity and the acceptor, oxoporphyrinogen entity, was found to be 1.61 V for the triad **5**.

To further understand the geometry and electronic structure of the triad **5**, computational studies using the B3LYP/3-21G(*) method[14] were performed. Figure 4 shows the optimized structure and the frontier HOMO and LUMO orbitals. The structure of the oxoporphyrinogen in **5** was found to be highly ruffled so that the β-pyrrole carbon displacement is as much as 1.7 Å from the macrocyclic least-

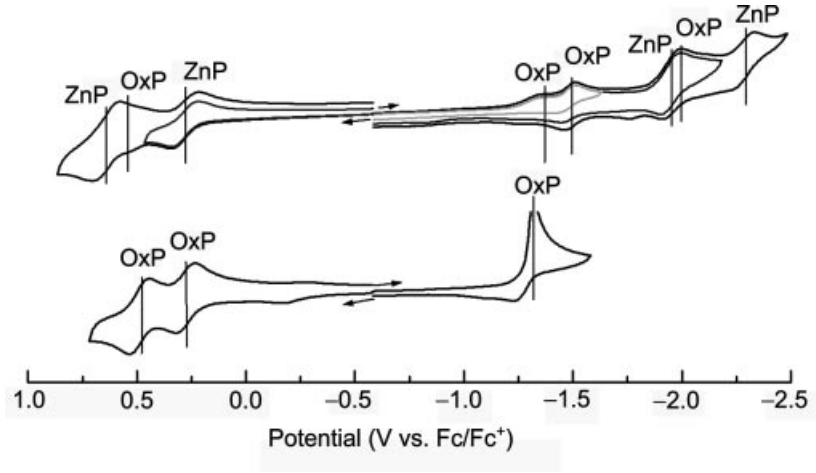

Figure 3. Cyclic voltammograms of (a) **5** (upper) and (b) **3** (lower) in *o*-dichlorobenzene containing 0.1 M $(\text{TBA})\text{ClO}_4$. Scan rate = 100 mV s^{-1}.

squares plane and this is in agreement with earlier X-ray and computational analyses of di-*N*-benzyl-substituted oxoporphyrinogens.[11,12] In the calculated structure, the intramolecular Zn–Zn distance is 18.6 Å while that between the Zn and the center of oxoporphyrinogen is 11.8 Å and there is no apparent association between the two zinc–porphyrins of **5**, a feature confirmed by the optical absorption data. The frontier HOMO was found located on a single zinc–porphyrin, as was predicted from the electrochemical data, and suggests a non-symmetric arrangement of the two ZnTPP moieties. On the other hand, the frontier LUMO was found localized on the oxoporphyrinogen entity so that the requirement of zinc–porphyrin as electron donor and oxoporphyrinogen as electron acceptor is fulfilled in the triad **5**. The B3LYP/3-21G(*)-computed HOMO–LUMO gap was found to be 1.83 eV, which is comparable with that deduced from electrochemical measurements.

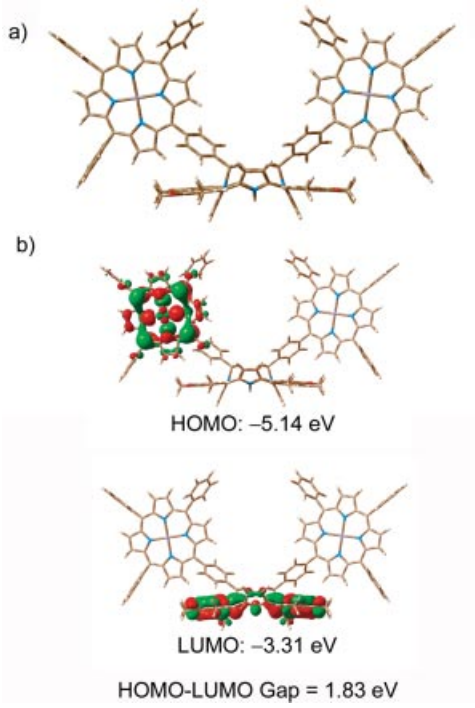

Figure 4. (a) B3LYP/3-21G(*)-optimized structure of triad, **5** and (b) the frontier HOMO and LUMO of the triad.

The free-energy changes for charge separation during generation of the radical ion-pair (ZnP)(Znp$^{\cdot+}$)-OxP$^{\cdot-}$ (ΔG^S_{CS}) were calculated according to Rehm and Weller[15] using the first oxidation potential of zinc–porphyrin, the first reduction potential of oxoporphyrinogen, the singlet excitation energy of the donor zinc–porphyrin, and the Coulomb energy (see Table 1, footnote for relevant equations). The ΔG^S_{CS} was found to be exothermic with a value of –0.58 eV in *o*-dichlorobenzene indicating the possibility of photoinduced electron transfer from a singlet excited zinc–porphyrin to the oxoporphyrinogen entity.

Preliminary steady-state fluorescence spectral studies were performed to understand the emission behaviour, and the results of these are shown in Figure 5, a. In *o*-dichlorobenzene, oxoporphyrinogen **3** is weakly fluorescent with

Table 1. Fluorescence lifetime, τ_f (collected at 580–650 nm), quenching rate-constant (k^S_q), quenching quantum-yield (Φ^S_q) of ^{1}ZnTPP* and free energy of charge-separation (ΔG^S_{CS}) of **5** (ZnTPP)$_2$-OxP) via ^{1}ZnTPP* generating (ZnTPP)(ZnTPP$^+$)-OxP$^{\cdot-}$.

Solvent	τ_f [ps]	$k^{S[a]}_q$ [s^{-1}]	$\Phi^{S[a]}_q$	$-\Delta G^S_{CS}$[b] [eV]
Benzonitrile	51	2.0×10^{10}	0.98	0.68
o-Dichlorobenzene	80	1.2×10^{10}	0.96	0.58
Toluene	104	1.0×10^{10}	0.95	0.05

[a] Lifetime (τ_f) of the reference compound ZnTPP was evaluated to be 2000 ps in toluene. The k^S_q and Φ^S_q were calculated from the differences in the fluorescence lifetimes between **5** and the reference compound. [b] Calculated from Rehm–Weller equations[15a] and employing ΔE_{0-0} = 2.07 eV for ^{1}ZnTPP*, E_{ox} = 0.28 V for ZnTPP, and E_{red} = –1.33 V for OxP vs. Fc/Fc$^+$ in *o*-dichlorobenzene. R^+ = 5.0 Å for ZnTPP, and R^- = 5.0 Å for OxP, and R_{CC} = 11.8 Å, for OxP-(ZnTPP)$_2$. Permittivities of toluene, *o*-dichlorobenzene, and benzonitrile, are 2.38, 9.93, and 25.2, respectively.

emission bands located at 609, 667 and 726 nm. The weak fluorescence of **3** can be attributed to the severe macrocyclic buckling and the quinonoid structure of the macrocycle.[16] Emission intensity due to the zinc–porphyrin entity in **5** is substantially quenched (> 95%) relative to pristine ZnTPP at the same concentration. Increasing the polarity of the solvent further increases the degree of emission-intensity quenching. The fluorescence spectra obtained after normalization of the ZnTPP fluorescence at 650 nm and measured by exciting selectively the ZnTPP moiety revealed emission bands corresponding to oxoporphyrinogen **3** at higher wavelengths, indicating the occurrence of Förster-type energy transfer as one of the ZnTPP-fluorescence quenching pathways. With increasing solvent polarity, fluorescence emission due to **3** decreased suggesting that charge-separation could also be contributing to the ZnTPP-fluorescence quenching (see Supporting Information; for details see the footnote on the first page of this article).

The time profile of pristine ZnTPP gives a mono-exponential decay with a lifetime of 1.95 ns. As expected, the time profile decay of the zinc–porphyrin emission in **5** is more rapid and exhibits biexponential decay with initial major short and minor long components (Figure 6, a). The lifetime of the minor long component is comparable to that of ZnTPP. Similar trends were also observed in solutions of **5** in toluene or benzonitrile. The lifetimes of the short-lived component of zinc–porphyrin in the triad are 104, 80, and 51 ps, in toluene, *o*-dichlorobenzene and benzonitrile, respectively.

The quenching rate and quantum yield calculated from the fluorescence decay at 600 nm in toluene are 1.0×10^{10} s^{-1} and 0.95, respectively (see Table 1, footnote for relevant equations and data in other solvents). The fluorescence quenching process in toluene can be attributed mostly to energy transfer because of an insufficient driving force for the charge-separation process in non-polar solvents (in toluene ΔG^S_{CS} = –0.05 eV in Table 1). Increasing the fluorescence decay rate with polarity of the solvent is interpreted

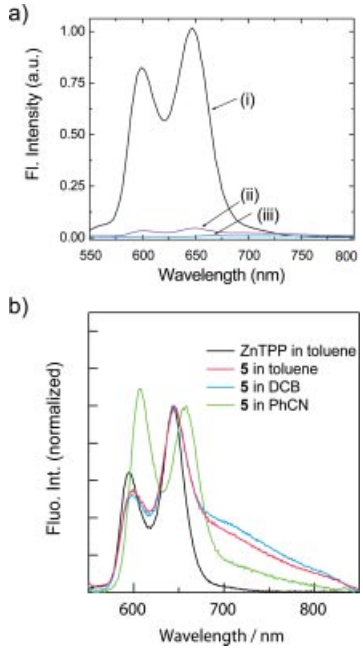

Figure 5. (a) Fluorescence spectra of (i) ZnTPP, (ii) **5** and (iii) **3** in *o*-dichlorobenzene. The concentrations held constant (except for OxP) at the Soret band. The samples were excited at the Soret band position of zinc–porphyrin in (i) and (ii), and at 536 nm in the case of **3**. (b) Normalized fluorescence spectra of ZnTPP and **5** in different solvents; λ_{ex} = 425 nm.

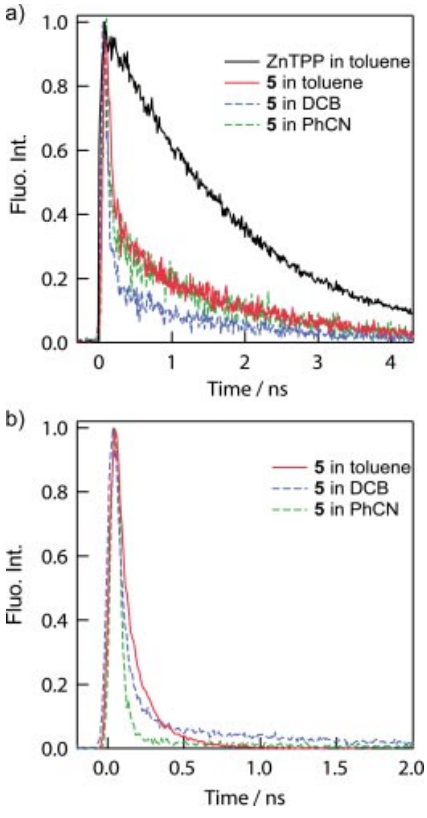

Figure 6. Fluorescence decay profiles of **5** (0.1 mM) collected over (a) the 600–640 nm range corresponding to zinc–porphyrin emission and (b) the 700–750 nm range for **3**; λ_{ex} = 410 nm.

in terms of the occurrence of a competing electron-transfer process in the more polar media based on the free energy calculations (ΔG^{S}_{CS} = –0.58 and –0.68 eV in *o*-dichlorobenzene and benzonitrile, respectively). The time profiles of the oxoporphyrinogen in **5**, in which the fast fluorescence decays were observed, are shown in Figure 6 (b). The initial rise corresponding to the energy-accepting process is not clear. Since these decay rates are similar to those for compound **3** (see Supporting Information), these short lifetimes of the excited states are likely an intrinsic characteristic of the oxoporphyrinogen moiety.

Compounds **3** and **5** were subjected to nanosecond transient absorption spectral measurements for characterization of the electron-transfer products. Nanosecond transient absorption spectra are shown in Figure 7 (a) for the triad **5** in toluene, which were obtained by the predominant excitation of the ZnTPP entity. Broad absorption bands were observed in the 600–1100 nm region with peak maxima around 830 nm. These absorptions are characteristic of the triplet states of ZnTPP[5c] and **3** (see Supporting Information, and this assignment is supported by their rapid decay in the presence of O_2. An initial increase in intensity at 860 nm in the time profile (right-hand side in Figure 7, a) may be due to the triplet energy-transfer from oxoporphyrinogen to ZnTPP.[5b,5c]

In a more polar solvent (benzonitrile), transient absorption spectra observed by the predominant excitation of the ZnTPP groups, revealed a weak absorption in the 600–1000 nm region (Figure 7, b), and suggest the occurrence of electron transfer as a competitive process with intersystem crossing for attenuation of generation of the triplet state of ZnTPP. It is likely that absorption bands corresponding to the radical ion-pair are obscured by the strong triplet absorptions, probably because of rapid charge-recombination rates. Similar transient absorption spectral behaviour was also observed in *o*-dichlorobenzene.

Figure 8 shows the energy-level diagram for the different photochemical events occurring in the triad. Emission and transient absorption studies demonstrate that upon excitation of the ZnTPP entity of **5** in toluene, energy transfer is the predominant photochemical process, and the anticipated electron-transfer process is not appreciable because of the lack of driving force. However, in polar solvents such as *o*-dichlorobenzene and benzonitrile, it is possible that an electron-transfer process occurs in competition with the energy-transfer process. The contribution due to electron transfer becomes greater with increasing solvent polarity because of an increase in the rate of that process.

The effect of solvent polarity on the formation and stability of charge-separated states is relatively well appreciated both in biochemical and synthetic systems.[18] It is interesting to note that, in the case of **5**, formation of a charge-separated state involves donation of an electron from an *N*-substituent (giving a zinc–porphyrin cation radical) to the oxoporphyrinogen. The resulting state of the oxoporphyrinogen moiety can be best described as an anion radical although it could be also formally seen as a porphyrinic cation radical. Such a tautology is in keeping with the

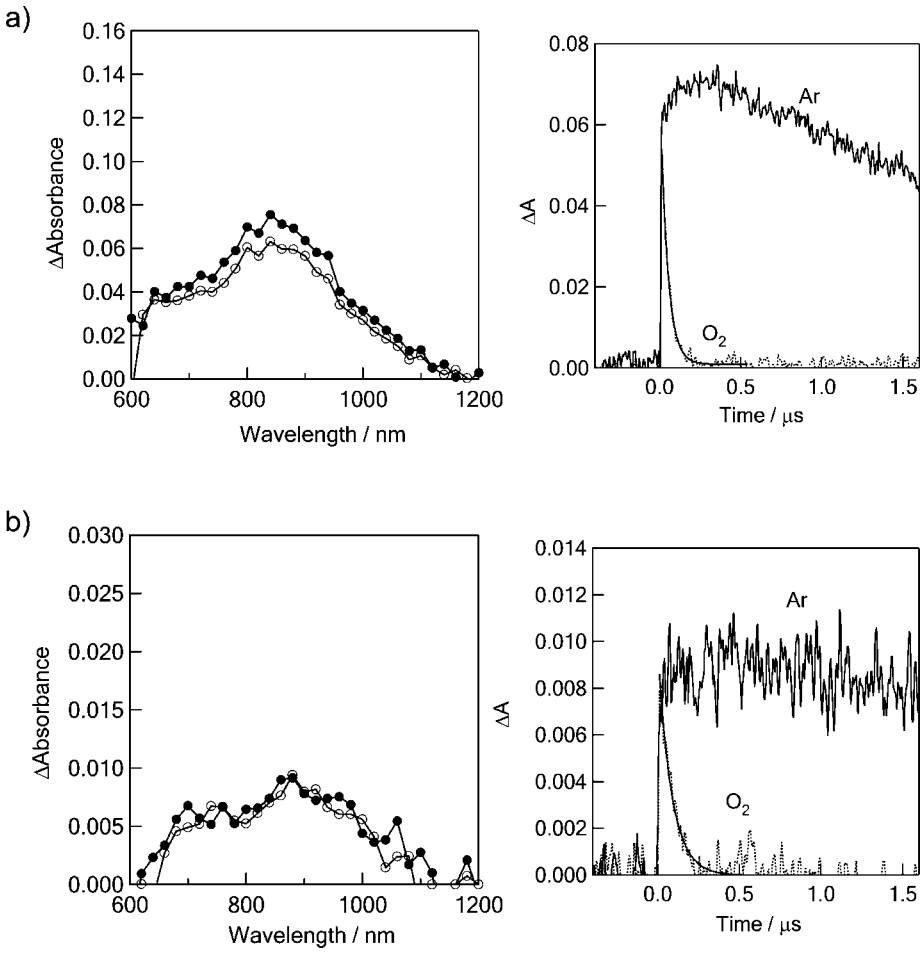

Figure 7. (a) Nanosecond transient absorption spectra of **5** (0.1 mM) observed by 425 nm laser irradiation for 0.1 μs (●) and 1.0 μs (○) in toluene. Right-hand side: Absorption-time profiles at 860 nm. (b) Nanosecond transient absorption spectra of **5** (0.1 mM) observed by 425 nm laser irradiation for 0.1 μs (●) and 1.0 μs (○) in benzonitrile. Right-hand side: Absorption-time profiles at 880 nm.

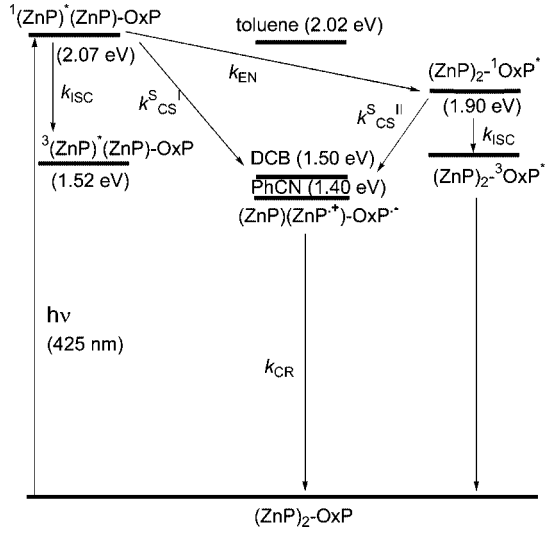

Figure 8. Energy level diagram showing the different photochemical events of triad **5**.

nature of the oxoporphyrinogen **3** and its parent porphyrin where the dual reactivities of porphyrin and antioxidant phenol substituents can be perplexing. Fortunately, *N*-alkylation of **3** allows distinction of its derivatives from the unsubstituted precursors. It is also significant that, in the *N*-substituted derivatives of **3**, intramolecular inter-substituent interaction is apparently not favoured because of the crowded environment at the core of the molecule and the restricted rotation about the bond between pyrrolic nitrogen atoms and substituent benzylic methylene. This arrangement could be of interest where a study of interaction between proximal but non-interacting chromophores is required.

In conclusion, we have prepared and studied an unprecedented example of a porphyrin-quinonoid featuring (tetraphenylporphinato)zinc(II) moieties covalently attached to an oxoporphyrinogen through the macrocyclic nitrogen atoms of the latter moiety. Optical absorption and computational studies reveal an absence of π–π-type interactions between the different chromophores of the triad. Free-energy calculations based on redox and emission data revealed

that electron transfer from the singlet-excited zinc–porphyrin to the oxoporphyrinogen is exothermic in polar solvents. The arrangement of chromophores in the triad results in an interesting interplay between the energy/electron-donating ZnTPP group(s) and the energy/electron-accepting tetrapyrrole-quinonoid as a function of solvent polarity. The compound described represents the most accessible of the porphyrin-oxoporphyrinogens and accounts of the properties of other similarly coupled derivatives, where we have attempted optimization for charge separation, will be reported shortly.

Experimental Section

All solvents and reagents were used as received. Reactions were performed under dry nitrogen. Size exclusion chromatography was performed using Biorad BioBeads SX-1. Tetra-*n*-butylammonium perchlorate, $(n\mathrm{Bu})_4\mathrm{NClO_4}$ was obtained from Fluka Chemicals. The synthesis of **3** was carried out according to published methods.[11]

Instrumentation: ^{1}H and ^{13}C NMR spectra were obtained from [D_1]-chloroform solutions using a JEOL AL300BX NMR spectrometer with tetramethylsilane as internal standard. MALDI-TOF mass spectroscopy was performed by Shimadzu Corp. The UV/Visible spectral measurements were carried out with a Shimadzu Model 1600 UV/Visible spectrophotometer. The fluorescence emission was monitored by using a Spex Fluorolog-tau spectrometer. Cyclic voltammograms were recorded with an EG&G Model 263A potentiostat using a three electrode system. A platinum button or glassy carbon electrode was used as the working electrode. A platinum wire served as the counter electrode and an Ag/AgCl was used as the reference electrode. Ferrocene/ferrocenium redox couple was used as an internal standard. All the solutions were purged prior to electrochemical and spectral measurements using argon gas. The computational calculations were performed by ab initio B3LYP/3-21G(*) methods with GAUSSIAN 03 software package[14] on high speed computers. The images of the frontier orbitals were generated from Gauss View-03 software.

Time-Resolved Emission and Transient Absorption Measurements: Picosecond time-resolved fluorescence spectra were measured using an argon-ion pumped Ti:sapphire laser (Tsunami) and a streak scope (Hamamatsu Photonics). Nanosecond transient absorption spectra in the near-IR region were measured by means of laser-flash photolysis; 532 nm light from a Nd:YAG laser was used as an exciting source and a Ge-avalanche-photodiode module was used for detection of the monitoring light from a pulsed Xe-lamp as described in our previous report.[21]

Syntheses

[5-(4-Bromomethylphenyl)-10,15,20-triphenylporphinato]zinc(II): This complex was prepared in three steps from the corresponding 5-(4-carboxymethylphenyl)-10,15,20-triphenylporphyrin (obtained by a mixed benzaldehyde condensation with pyrrole under Lindsey conditions[19]). Metallation of this unsymmetrically substituted porphyrin by the chloroform–methanol method[20] using zinc acetate tetrahydrate was followed by its reduction to the 4-(hydroxymethyl)phenyl derivative by treatment with lithium aluminium hydride in tetrahydrofuran and its subsequent conversion to the corresponding benzyl bromide using carbon tetrabromide/triphenylphosphane in tetrahydrofuran.

5-(4-Carboxymethylphenyl)-10,15,20-triphenylporphyrin: Trifluoroacetic acid (0.115 mL, 0.0015 mol) was added to a degassed mixture of pyrrole (1 g, 0.015 mol), benzaldehyde (1.06 g, 0.01 mol) and 4-(carboxymethyl)benzaldehyde (0.82 g, 0.005 mol) in dry dichloromethane (600 mL). The mixture was stirred at room temperature for 3 hours whereafter 2,3-dichloro-5,6-dicyanobenzoquinone (3.4 g, 0.015 mol) was added and the mixture was refluxed for 3 hours. After cooling, a few drops of triethylamine were added and the solvents were removed under reduced pressure. Initially, flash chromatography (SiO_2/CH_2Cl_2) was used to separate the porphyrinic products and this was followed by normal chromatography [SiO_2; gradient elution CH_2Cl_2/hexane (50:50) – CH_2Cl_2/hexane (60:40)] for separation of the required "mono-substituted" porphyrin, which was isolated as a purple amorphous powder. Yield: 0.28 g (11%). ^{1}H NMR ($CDCl_3$, 300 MHz): δ = –2.73 (s, 2 H), 4.10 (s, 3 H), 7.75 (m, 9 H), 8.20 (m, 6 H), 8.29 (d, ^3J = 8.26 Hz, 2 H), 8.42 (d, ^3J = 8.26 Hz, 2 H), 8.85–8.76 (m, 8 H) ppm. MALDI-TOF (dithranol) ($C_{46}H_{32}N_4O_2$): m/z = 672.72 $[M]^+$.

[5-(4-Hydroxymethylphenyl)-10,15,20-triphenylporphinato]zinc(II): 5-(4-Carboxymethylphenyl)-10,15,20-triphenylporphyrin (0.25 g, 3.7×10^{-4} mol) was dissolved in chloroform (50 mL) and zinc acetate dihydrate (0.24 g, 3 equiv., 0.011 mol) dissolved in methanol (10 mL) was added dropwise. The mixture was refluxed with stirring for 3 hours followed by removal of the solvents under reduced pressure. The zinc complex was purified by column chromatography over silica gel eluting with chloroform. After evaporation of solvents, the product was dried overnight under reduced pressure. Subsequently, the porphyrin was dissolved in dry tetrahydrofuran (10 mL) and added dropwise to a suspension of lithium aluminium hydride (20 mg, ≈ 1.5 equiv.) in dry tetrahydrofuran (20 mL). The mixture was stirred at room temperature until no starting material could be detected by thin layer chromatography (SiO_2/CH_2Cl_2). The mixture was poured carefully into water and then extracted with dichloromethane (2 × 50 mL). The organic phases were combined, then dried with anhydrous Na_2SO_4. Filtration and evaporation of the solvents gave the product as a red amorphous powder, which was dried under reduced pressure for 24 h and used without further purification. Yield (over two steps): 0.24 g (89%). ^{1}H NMR ($CDCl_3$, 300 MHz): δ = 4.96 (d, ^3J = 4.96 Hz, 2 H), 7.72 (m, 11 H), 8.20 (m, 8 H), 8.92 (m, 8 H) ppm. MALDI-TOF (dithranol) ($C_{45}H_{30}NOZn$): m/z = 704.75 $[M - H]^+$.

[5-(4-Bromomethylphenyl)-10,15,20-triphenylporphinato]zinc(II): An ice-cold suspension of carbon tetrabromide (170 mg, 5.1×10^{-4} mol) and triphenylphosphane (135 mg, 5.1×10^{-4} mol) in tetrahydrofuran (10 mL) was added slowly to an ice-cold solution of [5-(4-hydroxymethylphenyl)-10,15,20-triphenylporphinato]-zinc(II) (200 mg, 2.8×10^{-4} mol) in tetrahydrofuran (20 mL). The mixture was stirred until its composition was stationary (3–4 h) as determined by thin layer chromatography (SiO_2/CH_2Cl_2). The mixture was then poured into water and extracted with chloroform (2 × 50 mL). The organic phases were combined and dried with anhydrous Na_2SO_4. Filtration and evaporation of solvents gave a red solid, which was chromatographed over silica gel eluting with dichloromethane. Yield: 0.17 g (77%). ^{1}H NMR ($CDCl_3$, 300 MHz): δ = 4.87 (s, 2 H), 7.62 (d, ^3J = 7.87 Hz, 2 H), 7.74 (m, 7 H), 8.20 (m, 8 H), 8.91 (m, 8 H) ppm. MALDI-TOF (dithranol): m/z = 768.79 $[M + H]^+$.

Synthesis of 5: Compound **3** (50 mg, 4.5×10^{-5} mol) and [5-(4-bromomethylphenyl)-10,15,20-triphenylporphinato]zinc(II) (70 mg, 9.1×10^{-5} mol) were dissolved in dry dimethylformamide (5 mL) and anhydrous potassium carbonate (200 mg) was added. The mixture was stirred at 80 °C for 4–5 hours until consumption of the

bromomethyl-substituted porphyrin was apparent from thin layer chromatography. The reaction was poured into water and then extracted with dichloromethane (2 × 30 mL). The combined organic fractions were dried with anhydrous sodium sulfate. Filtration and removal of the solvents under reduced pressure was followed by column chromatography over silica gel eluting with dichloromethane/hexane gradient from 50:50 to 100:0. Compound **5** was collected as the highest yield fraction eluting after the low yield, higher substitution products. Further purification was affected by size exclusion chromatography eluting with tetrahydrofuran. The product was dried at room temperature under reduced pressure for 24 h. Yield: 75 mg (34%). ^{1}H NMR (C_6D_6, 300 MHz): δ = 1.12 [s, 36 H, C(CH_3)$_3$], 1.43 [s, 36 H, C(CH_3)$_3$], 5.09 (s, 4 H, benzylic CH_2), 6.78 (s, 4 H, cyclohexadienyl *H*), 7.15 (m, 4 H, cyclohexadienyl *H*, TPP phenyl *H*), 7.52 (s, 4 H, porphyrinogen β-pyrrolic *H*), 7.75 (m, 24 H, TPP phenyl *H*), 7.99 (d, ^3J = 8.08 Hz, 2 H, phenyl *H*), 8.16 (m, 6 H, phenyl *H*), 8.47 (d, ^3J = 4.77 Hz, 4 H, porphyrinic β-pyrrolic *H*), 8.58 (d, ^3J = 4.77 Hz, 4 H, porphyrinic β-pyrrolic *H*), 8.94 (m, 8 H, porphyrinic β-pyrrolic *H*), 10.04 (br. s, 2 H, N*H*) ppm. ^{13}C NMR (C_6D_6, 300 MHz): δ = 29.96, 30.16, 36.01, 36.25, 66.62, 118.69, 119.21, 120.34, 121.60, 121.66, 125.13, 125.33, 126.80, 126.92, 131.30, 131.44, 132.04, 132.34, 132.89, 134.63, 134.77, 135.82, 136.85, 137.22, 143.45, 143.57, 144.38, 148.34, 149.30, 149.99, 150.56, 150.57, 150.62, 186.04 ppm. MALDI-TOF (dithranol) ($C_{166}H_{148}N_{12}O_4Zn_2$): *m*/*z* = 2506.51 [M + H]$^+$.

Supporting Information Available (see footnote on the first page of this article): Steady-state fluorescence spectrum and transient absorption spectra of **3** in toluene.

Acknowledgments

The authors are thankful to the National Science Foundation (Grant 0453464 to F. D.), the donors of the Petroleum Research Fund administered by the American Chemical Society, and Grants-in-Aid for Scientific Research on Priority Area (417) from the Ministry of Education, Science, Sport and Culture of Japan (to O. I. and Y. A.). The authors are also grateful for support received from the Special Coordination Funds for Promoting Science and Technology from MEXT, Japan through an ICYS Fellowship (J. P. H.).

[1] a) J. Dalton, L. R. Milgrom, *J. Chem. Soc., Chem. Commun.* **1979**, 609–610; b) I. Tabushi, N. Koga, M. Yanagita, *Tetrahedron Lett.* **1979**, *20*, 257–260; c) A. D. Joran, B. A. Leland, G. G. Geller, J. J. Hopfield, P. B. Dervan, *J. Am. Chem. Soc.* **1984**, *106*, 6090–6092; d) D. Gust, T. A. Moore, in: *The Porphyrin Handbook* (Eds.: K. M. Kadish, K. M. Smith, R. Guilard), Academic Press: New York, **2000**, vol. 8, pp. 153–190; e) J. L. Sessler, M. R. Johnson, S. Creager, J. Fettinger, J. A. Ibers, *J. Am. Chem. Soc.* **1990**, *112*, 9310–9329; f) J. L. Sessler, M. R. Johnson, *Angew. Chem.* **1987**, *99*, 679–680; *Angew. Chem. Int. Ed. Engl.* **1987**, *26*, 678–680.

[2] a) S. L. Gould, G. Kodis, R. E. Palacios, L. de la Garza, A. Brune, D. Gust, T. A. Moore, A. L. Moore, *J. Phys. Chem. B* **2004**, *108*, 10566–10580; b) F. D′Souza, P. M. Smith, M. E. Zandler, A. L. McCarty, M. Itou, Y. Araki, O. Ito, *J. Am. Chem. Soc.* **2004**, *126*, 7898–7907; c) H. Kanato, K. Takimiya, T. Otsubo, Y. Aso, T. Nakamura, Y. Araki, O. Ito, *J. Org. Chem.* **2004**, *69*, 7183–7189; d) J. Andre′asson, G. Kodis, Y. Terazono, P. A. Liddell, S. Bandyopadhyay, R. H. Mitchell, T. A. Moore, A. L. Moore, D. Gust, *J. Am. Chem. Soc.* **2004**, *126*, 15926–15927; e) A. Berg, Z. Shuali, H. Levanon, A. Wiehe, H. Kurreck, *J. Phys. Chem. A* **2001**, *105*, 10060–10064.

[3] a) H. Dieks, M. O. Senge, B. Kirste, H. Kurreck, *J. Org. Chem.* **1997**, *62*, 8666–8680; b) M. Speck, H. Kurreck, M. O. Senge, *Eur. J. Org. Chem.* **2000**, *65*, 2303–2314; c) D. Gust, T. A. Moore, *Adv. Photochem.* **1991**, *16*, 1–65; d) M. R. Wasielewski, *Chem. Rev.* **1992**, *92*, 435–461; e) H. Kurreck, M. Huber, *Angew. Chem.* **1995**, *107*, 929–947; *Angew. Chem. Int. Ed. Engl.* **1995**, *34*, 849–866; f) J. S. Connolly, J. R. Bolton, in: *Photoinduced Electron Transfer Part D* (Eds.: M. A. Fox, M. Chanon), Elsevier, Amsterdam, **1988**, pp. 303–393; g) S. Nishitani, N. Kurata, Y. Sakata, S. Misumi, A. Karen, T. Okada, N. Mataga, *J. Am. Chem. Soc.* **1983**, *105*, 7771–7772; h) D. Gust, T. A. Moore, A. L. Moore, D. Barrett, L. O. Harding, L. R. Makings, P. A. Liddell, F. C. de Schryver, M. van der Auweraer, R. V. Bensasson, M. Rougée, *J. Am. Chem. Soc.* **1988**, *110*, 321–323; i) D. Gust, T. A. Moore, A. L. Moore, S.-J. Lee, E. Bittersmann, D. K. Luttrull, A. A. Rehms, J. M. DeGraziano, X. C. Ma, F. Gao, R. E. Belford, T. T. Trier, *Science* **1990**, *248*, 199–201; j) O. Korth, A. Wiehe, H. Kurreck, B. Roeder, *Chem. Phys.* **1999**, *246*, 363–372; k) G. Li, S. V. Bhosale, T. Wang, S. Hackbarth, B. Roeder, U. Siggel, J.-H. Fuhrhop, *J. Am. Chem. Soc.* **2003**, *125*, 10693–10702; l) A. Harriman, J.-P. Sauvage, *Chem. Soc. Rev.* **1996**, *25*, 41–48; m) M.-J. Blanco, M. C. Jiménez, J.-C. Chambron, V. Heitz, M. Linke, J.-P. Sauvage, *Chem. Soc. Rev.* **1999**, *28*, 293; n) V. Balzani, A. Juris, M. Venturi, S. Campagna, S. Serroni, *Chem. Rev.* **1996**, *96*, 759; o) *Electron Transfer in Chemistry* (Ed.: V. Balzani); Wiley-VCH: Weinheim, **2001**; p) M. N. Paddon-Row, *Acc. Chem. Res.* **1994**, *27*, 18; q) J. W. Verhoeven, *Adv. Chem. Phys.* **1999**, *106*, 603; r) K. Maruyama, A. Osuka, N. Mataga, *Pure Appl. Chem.* **1994**, *66*, 867; s) A. Osuka, N. Mataga, T. Okada, *Pure Appl. Chem.* **1997**, *69*, 797; t) J. S. Sessler, B. Wang, S. L. Springs, C. T. Brown, in: *Comprehensive Supramolecular Chemistry* (Eds.: J. L. Atwood, J. E. D. Davies, D. D. MacNicol, F. Vögtle), Chapter 9, Pergamon, **1996**; u) T. Hayashi, H. Ogoshi, *Chem. Soc. Rev.* **1997**, *26*, 355; v) M. W. Ward, *Chem. Soc. Rev.* **1997**, *26*, 365; w) J. L. Sessler, M. R. Johnson, T.-Y. Lin, S. Creager, *J. Am. Chem. Soc.* **1988**, *110*, 3659–3661.

[4] a) D. Mauzerall, in: *The Porphyrins* (Eds.: D. Dolphin), Academic Press: New York, **1978**, vol. V, part C, pp. 29–52; b) Y. K. Kang, I. V. Rubtsov, P. M. Iovine, J. Chen, M. J. Therien, *J. Am. Chem. Soc.* **2002**, *124*, 8275–8279; c) H. A. Staab, R. Hauck, A. Feurer, *Angew. Chem. Int. Ed.* **1994**, *33*, 24–28.

[5] a) H. Imahori, Y. Sakata, *Eur. J. Org. Chem.* **1999**, 2445–2457; b) F. D′Souza, G. R. Deviprasad, M. E. El-Khouly, M. Fujitsuka, O. Ito, *J. Am. Chem. Soc.* **2001**, *123*, 5277–5284; c) F. D′Souza, G. R. Deviprasad, M. E. Zandler, M. E. El-Khouly, M. Fujitsuka, O. Ito, *J. Phys. Chem. B* **2002**, *106*, 4952–4962; d) K. Li, P. J. Bracher, D. M. Guldi, M. A. Herranz, L. Echegoyen, D. I. Schuster, *J. Am. Chem. Soc.* **2004**, *126*, 9156–9157; e) D. M. Guldi, C. Luo, M. Prato, A. Troisi, F. Zerbetto, M. Scheloske, E. Dietel, W. Bauer, A. Hirsch, *J. Am. Chem. Soc.* **2001**, *123*, 9166–9167; f) S. Fukuzumi, H. Imahori, H. Yamada, M. E. El-Khouly, M. Fujitsuka, O. Ito, D. M. Guldi, *J. Am. Chem. Soc.* **2001**, *123*, 2571–2575; g) N. Martín, L. Sánchez, B. Illescas, I. Pérez, *Chem. Rev.* **1998**, *98*, 2527; h) D. M. Guldi, *Chem. Commun.* **2000**, 321; i) D. M. Guldi, *Chem. Soc. Rev.* **2002**, *31*, 22; j) M. D. Meijer, G. P. M. van Klink, G. van Koten, *Coord. Chem. Rev.* **2002**, *230*, 141; k) M. E. El-Khouly, O. Ito, P. M. Smith, F. D′Souza, *J. Photochem. Photobiol. C.* **2004**, *5*, 79; l) H. Imahori, S. Fukuzumi, *Adv. Funct. Mater.* **2004**, *14*, 525.

[6] a) Q. Xie, E. Pèrez-Cordero, L. Echegoyen, *J. Am. Chem. Soc.* **1992**, *114*, 3978–3979; b) M. Bendikov, F. Wudl, D. F. Perepichka, *Chem. Rev.* **2004**, *104*, 4891–4945.

[7] a) P. A. Liddell, G. Kodis, A. L. Moore, T. A. Moore, D. Gust, *J. Am. Chem. Soc.* **2002**, *124*, 7668–7669; b) S. D. Straight, J. Andréasson, G. Kodis, A. L. Moore, T. A. Moore, D. Gust, *J. Am. Chem. Soc.* **2005**, *127*, 2717–2724; c) R. A. Bissell, A. P. de Silva, H. N. Gunaratne, P. M. Lynch, G. E. Maguire, K. S. Sandanayake, *Chem. Rev.* **1992**, *92*, 7–195; d) C. A. Mirkin, M. A. Ratner, *Annu. Rev. Phys. Chem.* **1992**, *43*, 719–754; e) H. Shiratori, T. Ohno, K. Nozaki, I. Yamazaki, Y. Nishimura, A.

Osuka, *Chem. Commun.* **1998**, 1539–1540; f) *Introduction to Molecular Electronics* (Eds.: M. C. Petty, M. R. Bryce, D. Bloor), Oxford University Press, New York, **1995**; g) *Molecular Switches* (Ed.: B. L. Feringa), Wiley-VCH, Weinheim, **2001**.
[8] C. Otto, E. Breitmaier, *Liebigs Ann. Chem.* **1991**, 1347.
[9] H. H. Inhoffen, J.-H. Fuhrhop, F. van der Haar, *Justus Liebigs Ann. Chem.* **1966**, *700*, 92–105.
[10] L. R. Milgrom, J. P. Hill, G. Yahioglu, *J. Heterocycl. Chem.* **1995**, *32*, 97–101.
[11] J. P. Hill, I. J. Hewitt, C. E. Anson, A. K. Powell, A. L. McCarty, P. A. Karr, M. E. Zandler, F. D′Souza, *J. Org. Chem.* **2004**, *69*, 5861–5869.
[12] J. P. Hill, W. Schmitt, A. L. McCarty, K. Ariga, F. D′Souza, *Eur. J. Org. Chem.* **2005**, 2893–2902.
[13] E. Dolušić, S. Toppet, S. Smeets, L. V. Meervelt, B. Tinant, W. Dehaen, *Tetrahedron* **2003**, *59*, 395–400.
[14] *Gaussian 03* (Revision B-04), Gaussian, Inc., Pittsburgh PA, **2003**.
[15] a) D. Rehm, A. Weller, *Isr. J. Chem.* **1970**, *8*, 159–271; b) N. Mataga, H. Miyasaka, in: *Electron Transfer* (Eds.: J. Jortner, M. Bixon), John Wiley & Sons: New York, **1999**, part 2, pp. 431–496.
[16] It is known that the fluorescence quantum yield and lifetime of porphyrins decrease with increasing nonplanarity of the porphyrin macrocycle (see ref.[17]).
[17] a) S. Gentemann, N. Y. Nelson, L. Jaquinod, D. J. Nurco, S. H. Leung, C. J. Medforth, K. M. Smith, J. Fajer, D. Holten, *J. Phys. Chem. B* **1997**, *101*, 1247; b) I. V. Sazanovich, V. A. Galievsky, A. van Hoek, T. J. Schaafsma, V. L. Malinovskii, D. Holten, V. S. Chirvony, *J. Phys. Chem. B* **2001**, *105*, 7818.
[18] a) M. Bixon, J. Jortner, *Adv. Chem. Phys.* **1999**, *106*, 35–202; b) *Photoinduced Electron Transfer* (Eds.: M. A. Fox, M. Chanon), parts A–D, Elsevier, Amsterdam, **1988**.
[19] J. S. Lindsey, I. C. Schreiman, H. C. Hsu, P. C. Kearney, A. M. Marguerettaz, *J. Org. Chem.* **1987**, *52*, 827.
[20] *Porphyrins and Metalloporphyrins* (Ed.: K. M. Smith), Elsevier, Amsterdam, **1975**.
[21] a) K. Matsumoto, M. Fujitsuka, T. Sato, S. Onodera, O. Ito, *J. Phys. Chem. B.* **2000**, *104*, 11632; b) S. Komamine, M. Fujitsuka, O. Ito, K. Morikawa, T. Miyata, T. Ohno, *J. Phys. Chem. A.* **2000**, *104*, 11497; c) M. Yamazaki, Y. Araki, M. Fujitsuka, O. Ito, *J. Phys. Chem. A* **2001**, *105*, 8615.

Received: August 18, 2005
Published Online: October 12, 2005

